

# Formation of galaxies and large-scale structure with cold dark matter

George R. Blumenthal\* & S. M. Faber\*

\* Lick Observatory, Board of Studies in Astronomy and Astrophysics, University of California, Santa Cruz, California 95064, USA

Joel R. Primack<sup>†§</sup> & Martin J. Rees<sup>‡§</sup>

<sup>†</sup> Stanford Linear Accelerator Center, Stanford University, Stanford, California 94305, USA

<sup>‡</sup> Institute of Theoretical Physics, University of California, Santa Barbara, California 93106, USA

*The dark matter that appears to be gravitationally dominant on all scales larger than galactic cores may consist of axions, stable photinos, or other collisionless particles whose velocity dispersion in the early Universe is so small that fluctuations of galactic size or larger are not damped by free streaming. An attractive feature of this cold dark matter hypothesis is its considerable predictive power: the post-recombination fluctuation spectrum is calculable, and it in turn governs the formation of galaxies and clusters. Good agreement with the data is obtained for a Zeldovich ( $|\delta_k|^2 \propto k$ ) spectrum of primordial fluctuations.*

WHY are there galaxies, and why do they have the sizes and shapes that we observe? Why are galaxies clustered hierarchically in clusters and superclusters, separated by enormous voids in which bright galaxies are almost entirely absent? And what is the nature of the invisible mass, or dark matter, that we detect gravitationally roundabout galaxies and clusters but cannot see directly in any wavelength of electromagnetic radiation? Of the great mysteries of modern cosmology, these three may now be among the ripest for solution.

Because there is evidence that the mass of dark matter in the Universe exceeds that of the visible matter by at least an order of magnitude<sup>1</sup>, the third question may hold the key to the first two. We now consider the hypothesis that the dark matter is cold<sup>2-7</sup>, that is, that its thermal velocity is cosmologically negligible in the early Universe.

Most modern theories of the origin of structure in the Universe assume that the extreme inhomogeneity of the present Universe grew gravitationally from initially very small density fluctuations<sup>8,9</sup>. One hypothesis extensively explored<sup>10-12</sup> is that the dark matter (DM) consists of neutrinos of mass  $\sim 30$  eV. Because these particles are noninteracting for  $t \geq 1$  s but are still relativistic at  $t \sim 1$  yr when galaxy-size masses first come within the horizon ( $R_{\text{horizon}} = ct$ ), they would freely stream away, smoothing out fluctuations of horizon size or smaller. We refer to such particles as hot DM, and to the phenomenon just mentioned as damping by free streaming. The mass of the neutrinos inside the horizon when they first become nonrelativistic is roughly  $10^{15} M_{\odot}$ , about the mass of a supercluster ( $M_{\odot}$  is the solar mass). This is consequently the mass of the first structures to collapse gravitationally in a neutrino-dominated Universe.

It is also possible that the DM consists of elementary particles that decoupled thermally from the big bang much earlier than neutrinos. It can be shown that such particles would have lower number density today, and thus could be more massive ( $\sim 1$  keV) and become nonrelativistic sooner than neutrinos<sup>13,14</sup>. We refer to this as warm DM. The first structures to form in such a Universe would weigh about  $10^{11} M_{\odot}$ , about the mass of a typical galaxy<sup>15-17</sup>.

In contrast, in a Universe dominated by cold DM, the free streaming damping mass is, by definition, smaller than galaxy masses. Below, we will discuss possible particle physics candidates for cold DM and explain why we believe it is more

plausible that the Universe is dominated gravitationally by cold DM than by ordinary matter (baryons) or hot or warm DM. We next consider galaxy formation in the cold DM picture, and show that galaxy and cluster data compare favourably with the predictions of this model. We then discuss the extent to which the data constrain the cosmological density in the cold DM picture, and the evolution of superclusters and voids. The cold DM hypothesis seems to lead to a remarkably attractive theory for galaxy formation and to account for large-scale structure at least as well as any competing theory.

## Evidence that dark matter is cold

Cold DM consists of particles having negligible thermal velocity with respect to the Hubble flow and having nongravitational interactions that are much weaker than the weak interactions<sup>3,4</sup>. A popular cold DM candidate is the axion<sup>18</sup>, a pseudoscalar field proposed originally to avoid large CP (constant parity) violation in the strong interactions (which would imply, for example, much too large a value for the neutron electric dipole moment)<sup>19-21</sup>. Instanton effects generate a nonzero axion mass at the quark deconfinement temperature ( $T \sim 10^2$  MeV), below which the axions act as a nonrelativistic, massive, pressureless fluid. The requirement that the axion density be less than the critical density implies that the axion mass  $m_a \geq 10^{-5}$  eV (refs 22-24), while the longevity of helium burning stars implies that  $m_a < 10^{-1}$  eV (ref. 25). Thus, if axions exist, they may be cosmologically important, and, for  $m_a \approx 10^{-5}$  eV, they would be gravitationally dominant. If axions comprise the dark halo of our Galaxy, laboratory experiments have recently been proposed that could detect them<sup>26</sup>.

Another cold DM candidate particle is the photino, the spin  $\frac{1}{2}$  supersymmetric partner of the photon. Photinos are thought to be the lightest supersymmetric particle, with  $m_{\tilde{\nu}} \geq 0.5$  GeV (the lower limit corresponding to cosmological critical density)<sup>27</sup>. As photino annihilation at high temperatures is incomplete, the remnant photinos can, because of their large mass, contribute a critical density today.

A third cold DM candidate is black holes<sup>28,29</sup> of mass  $10^{-16} M_{\odot} \leq M_{\text{BH}} \leq 10^6 M_{\odot}$ , the lower limit implied by the non-observation of  $\gamma$  rays from black hole decay by Hawking radiation, and the upper limit required to avoid disruption of galactic disks and star clusters<sup>30,31</sup>. Stronger but more controversial upper limits are  $M_{\text{BH}} < 10^2 M_{\odot}$  from dwarf spheroidal haloes<sup>32</sup> and  $M_{\text{BH}} < 10^{-2} M_{\odot}$  from the non-observation of focusing of quasar cores<sup>33</sup>.

§ Permanent addresses: Santa Cruz Institute of Particle Physics, University of California, Santa Cruz, California 95064, USA (J.R.P.); Institute of Astronomy, Madingley Road, Cambridge CB3 0HA, UK (M.J.R.).

Another exotic cold DM candidate, recently proposed by Witten, is "nuggets" of  $u$ - $s$ - $d$  symmetric quark matter<sup>34</sup>. There is thus no shortage of cold DM candidate particles—although there is no direct evidence that any of them actually exists. Our motivation for considering the hypothesis that the Universe is dominated by cold DM is twofold. First, there is more than a little evidence against baryonic, hot, and warm DM. Moreover, a cold DM Universe correctly predicts many of the observed properties of galaxies, including their range of masses, irrespective of the identity of the cold particle.

The most conventional assumption might be that DM is baryonic, since we know that baryons pervade the Universe. There are, however, three arguments that make a nonbaryonic form of DM more plausible. First, if DM consists of baryons, it must be clumped into objects with mass  $\ll M_{\odot}$  to avoid nuclear burning and the emission of too much radiation<sup>35</sup>, and there is no compelling theory for the formation of such a large density of objects of planetary mass or smaller. The difficulties with other possible forms of baryonic dark matter have been reviewed elsewhere<sup>36</sup>. The second argument involves the observed deuterium abundance,  $D/H = (1-4) \times 10^{-5}$  (by number), which provides a lower limit on the primordial D abundance because deuterium is readily consumed but not produced in stars. This then corresponds to an upper limit for the baryonic density parameter (ratio of baryon density to critical density) of  $\Omega_b \leq 0.035 h^{-2} (T_0/2.7)^3$  (ref. 37), where  $T_0$  is the present temperature of the microwave background radiation and  $h$  is Hubble's constant expressed in units of  $100 \text{ km s}^{-1} \text{ Mpc}$ . (Observationally,  $1/2 \leq h \leq 1$ .) However, there is also strong observational evidence that the total density parameter  $\Omega \geq 0.1$ . Therefore a baryon dominated Universe ( $\Omega = \Omega_b$ ) is consistent with the deuterium limit only for  $\Omega$  and  $h$  very near their observational lower limits. Finally, the existence of galaxies and clusters today requires that perturbations in the density must have become nonlinear before the present epoch. In a baryonic Universe, for adiabatic perturbations at recombination, this implies present-day fluctuations in the microwave background much larger than the present observational upper limits<sup>38,39</sup>. For baryonic DM, this problem can be avoided if the primordial fluctuation spectrum is isothermal rather than adiabatic, contrary to grand unified models of baryosynthesis<sup>40,41</sup>, or if there is significant reheating of the intergalactic medium after recombination<sup>42</sup>. For nonbaryonic DM, on the other hand, the predicted fluctuations in the microwave background can be consistent with the observations as the fluctuations in the baryon-photon fluid are small at recombination and only later grow to the same size as fluctuations in the DM.

The neutrino dominated picture of galaxy formation also has serious weaknesses. Studies of nonlinear clustering (on scales  $\lambda < 10 \text{ Mpc}$ ) show that supercluster collapse must have occurred quite recently, at redshift  $z_{sc} < 2$  (refs 43, 44). This is also consistent with a study of streaming velocity in the linear regime ( $\lambda > 10 \text{ Mpc}$ ), which indicates  $z_{sc} < 0.5$  (ref. 45). However, the best limits on galaxy ages coming from globular clusters and other stellar populations, plus the possible association of QSOs with galactic nuclei, indicate that galaxy formation took place before  $z = 3$  (ref. 46). This is inconsistent with the neutrino 'top-down' theory, in which superclusters form before galaxies rather than after them.

Another problem with the neutrino picture is that large clusters of galaxies can accrete neutrinos more efficiently than ordinary galactic haloes, which have lower escape velocities. One-dimensional numerical simulations predict that the ratio of total-to-baryonic mass  $M/M_b$  should be  $\sim 5$  times larger for clusters ( $\sim 10^{14} M_{\odot}$ ) than for ordinary galaxies ( $M \sim 10^{12} M_{\odot}$ )<sup>47</sup>. While there is evidence that mass-to-light ratio  $M/L$  does increase with scale, there is also considerable evidence that the more physically meaningful ratio of total-to-luminous mass  $M/M_{lum}$  remains constant from large clusters through groups of galaxies, binary galaxies, and ordinary spirals. ( $M_{lum}$ , which is the mass visible in galactic stars and gas plus hot, X-ray emitting gas, is  $\leq M_b$ , as an unknown fraction of the baryons is

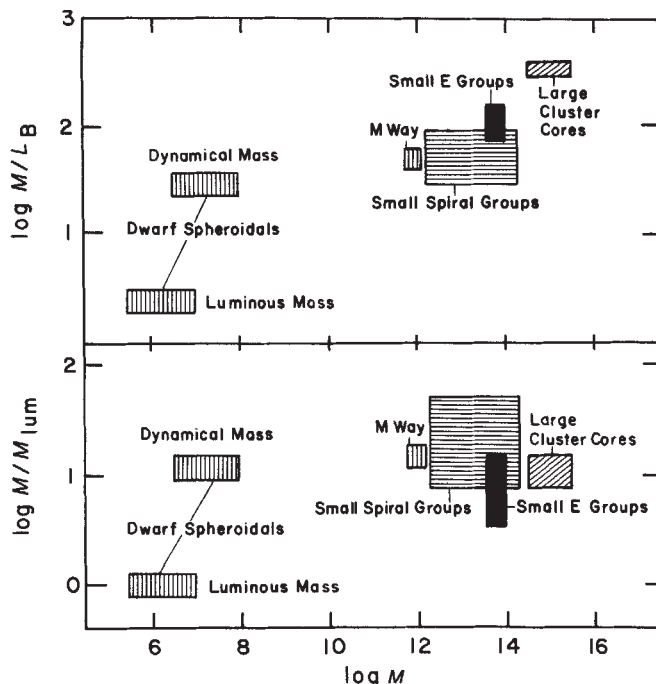


Fig. 1 Mass-to-light ratio,  $M/L_B$ , and total-to-luminous mass,  $M/M_{lum}$ , for structures of various size in the Universe. The data come from Table 1. Although  $M/L_B$  increases systematically with mass, the more physically meaningful ratio  $M/M_{lum}$  appears to be constant on all scales within the errors. If the velocity dispersion data for the dwarf spheroidal galaxies are interpreted to imply heavy haloes, the upper estimates result. The lower estimates follow from assuming that all the mass is visible. We believe the former estimate to be more realistic.

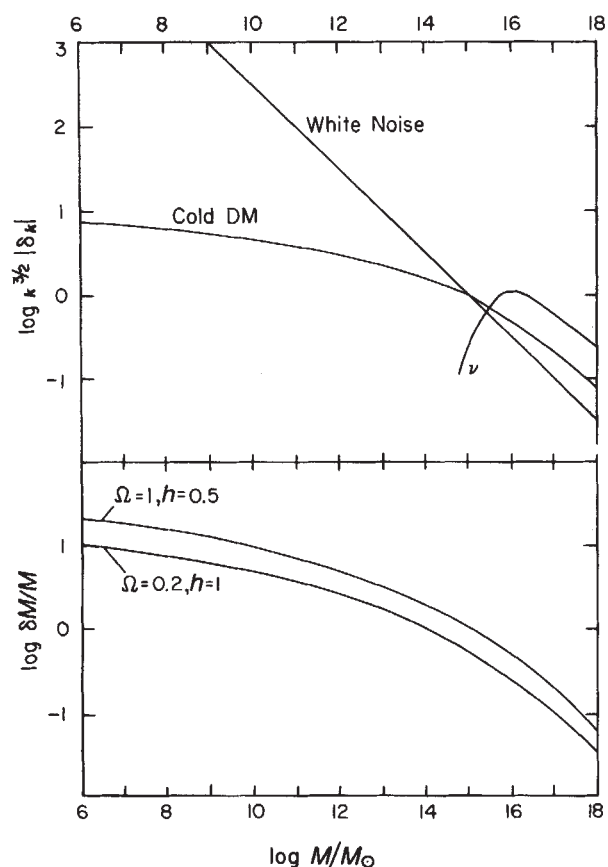


Fig. 2 Density fluctuations as a function of mass.  $a, k^{3/2} |\delta_k| = \delta\rho/\rho(M)$ , where  $M = 4\pi^2 \rho_0 / 3k^3$ , for isothermal white noise ( $n=0$ ), and adiabatic Zeldovich ( $n=1$ ) neutrino<sup>16</sup> and cold DM spectra.  $b$ , r.m.s. mass fluctuation within a randomly placed sphere containing mass  $M$  for cold DM,  $n=1$ , and ( $\Omega=1, h=0.5$ ), ( $\Omega=0.2, h=1$ ).

invisible—for example, in the form of diffuse ionized intergalactic gas at  $T \sim 10^4$  K.) This is illustrated in Table 1 and Fig. 1, where we have plotted observed data for  $M/L$  and  $M/M_{\text{lum}}$ . The fact that the total-to-luminous mass of rich clusters is similar to that of galaxies including their massive haloes, even though the clusters' mass-to-light ratio is larger, is due mainly to the different stellar population in the E and S0 galaxies in rich clusters plus the large contribution of X-ray emitting gas to  $M_{\text{lum}}$ . In very rich clusters such as Coma, there is perhaps  $\sim 2$ – $5$  times as much mass in hot gas as there is in stars.

Finally, preliminary velocity dispersion data for Draco, Carina, and Ursa Minor<sup>48–50</sup> as well as theoretical arguments<sup>51</sup> suggest that a significant amount of DM may reside in dwarf spheroidal galaxies. Because of the low velocity dispersion of dwarf galaxies, phase space constraints give a lower limit of  $m > 500$  eV for the mass of particles comprising this DM<sup>32</sup>. The present velocity dispersion estimates are uncertain owing to possible stellar oscillations, mass outflow, and binary motions, but these effects can be discovered and eliminated with careful monitoring. Taken at face value, however, the existing mass limit of 500 eV would rule out neutrinos completely.

Although warm DM provides a natural (free streaming) scale for ordinary galaxies, it cannot account for massive haloes in dwarf spheroidals even though the warm DM mass is actually, if barely, consistent with the phase space constraint. This is because free streaming damps out fluctuations with mass  $< 10^{11} M_{\odot}$ , so dwarf galaxies with mass  $\sim 10^7 M_{\odot}$  can form in this picture only by the fragmentation of much larger scale galactic masses. Because dwarf galaxies with escape velocity  $\sim 10 \text{ km s}^{-1}$  would capture only a small fraction of the warm DM particles, whose velocity dispersion would be  $\sim 100 \text{ km s}^{-1}$ , typical of ordinary spirals, one would expect  $M/M_{\text{lum}}$  to be much smaller in dwarf galaxies than in spirals. However, the dynamical mass data on dwarf spheroidals shown in Fig. 1 suggest a similar value for the ratio of total-to-luminous mass. In view of the great importance of dwarf spheroidal haloes to constraints on warm as well as hot DM, it is clearly urgent to continue the monitoring programme on velocity dispersions mentioned above.

Recently proposed models having two or more kinds of possibly unstable DM<sup>52–58</sup> may be easier to reconcile with observations than models with one stable DM species, in part because of their additional adjustable parameters. Such models are, however, beyond the scope of this paper.

## Galaxy formation with cold dark matter

The key features of galaxy formation in the cold DM picture are these: the DM fluctuation spectrum at recombination is determined by a small number of physical parameters; after recombination (at  $z_{\text{rec}} \approx 1,300$ ) the amplitude of the baryonic fluctuations rapidly grows to match that of the DM fluctuations; smaller-mass fluctuations grow to nonlinearity and virialize, and then are hierarchically clustered within successively larger bound systems; and finally the ordinary matter in bound systems of total mass  $\sim 10^{8-12} M_{\odot}$  cools rapidly enough within the DM haloes to form galaxies, while larger mass fluctuations form clusters.

To calculate the growth of initially small perturbations and their ultimate gravitational collapse into condensed systems, one must first determine an initial spectrum for density perturbations in the very early Universe. We assume here that the initial fluctuations are adiabatic, which is consistent with fashionable particle theories in which a small excess of baryons over antibaryons is generated by the decay of supermassive grand unified theory particles<sup>40,41</sup>. Then the mass (or energy) density at any point can be written as  $\rho(r, t) = \rho_0(1 + \delta)$ , where  $\rho_0(t)$  is the average density in the Universe and  $\delta$  represents the fractional density perturbation in the synchronous gauge. If the fluctuation spectrum is characterized by a power law distribution, then the r.m.s. fluctuation on mass scale  $M$  can be written  $\delta \propto M^{(-1/2) - (n/6)}$ , which corresponds to a Fourier power spectrum  $|\delta_k|^2 \propto k^n$ . Alternatively, we can characterize the perturbations

Table 1  $M/L_B$  and  $M/M_{\text{lum}}$  on various mass scales

Unit	$M^*$	$M/L_B^\dagger$	$M_{\text{gas}}/M_{\text{lum}}^\ddagger$	$M/M_{\text{lum}}$
Large clusters	$10^{15} M_{\odot}$	$316 \pm 40^\ddagger$	$0.84^{+0.0}{}^\S$	$8.4^{+7.0}{}_{-1.0}$
Small E-dominated groups	$5 \times 10^{13}$	$83^{+80}{}_{-10}^\ddagger$	$0.61^{+0.1}{}_{-0.1}^\S$	$5.4^{+10.0}{}_{-2.0}^\#$
Small spiral-dominated groups	$2 \times 10^{13}$	$40^{+50}{}_{-10}^\ddagger$	0(?)	$14.2^{+36}{}_{-6}^\#$
Whole Milky Way	$10^{12} M_{\odot}$	$50^\ddagger$	0(?)	$14^\ddagger$
Dwarf spheroidals $^\S$				
Stellar masses	$10^{5-7}$	2.5	0	1
Dynamical masses	$10^{6-8}$	30	0	12

\* Total mass including dark matter.  $H = 50 \text{ km s}^{-1} \text{ Mpc}$ .

† Mass-to-light ratio on B(0) magnitude system as described in ref. 1.

‡ From ref. 120.

§  $M_{\text{gas}}/M_{\text{lum}}$  is calculated as the product of two factors:  $(M_{\text{gas}}/M) \times (M_{\text{lum}}/M)^{-1}$ .  $M_{\text{gas}}/M = 0.10^{+0.02}{}_{-0.05}$  from ref. 121 for 14 X-ray clusters. Formal clusters have been increased to allow for the unknown gas distribution outside the core and possible settling of gas relative to galaxies or vice versa.  $M_{\text{lum}}/M$  is  $(M_{\text{star}} + M_{\text{gas}})/M$ , where  $M_{\text{star}}/M$  is the fractional mass in stars. It may be calculated as  $(M/L_B)_{\text{star}}(M/L_B)^{-1}$ , where  $(M/L_B)_{\text{star}}$  is the stellar mass-to-light ratio. For E and S0 galaxies in large clusters,  $(M/L_B)_{\text{star}}$  appears to be about 6 (ref. 1).

¶  $L_V$ ,  $M_{\text{gas}}$ , and  $M$  from ref. 122 based on five groups.  $L_V$  corrected to B(0) system based on data provided by Kriss (personal communication). Comparison with Beers *et al.*<sup>123</sup> suggests that  $M$  may be underestimated by a factor of two. Quoted errors take this into account.

‡ From ref. 1.

¶ From ref. 72; includes baryonic mass in stars and neutral gas.

\*\* Mass assumed to be 1/3 total mass of Local Group<sup>1</sup>.

†† B(0) luminosity from ref. 1.

‡‡  $M_{\text{lum}}$  from ref. 124.

§§ Basic data from ref. 51. Upper line assumes that only stars are present. Lower line includes excess dark matter, based on mean dynamical masses of Faber and Lin<sup>51</sup> and Aaronson *et al.*<sup>48–50</sup>.

on mass scale  $M$  when that mass scale crosses (first comes within) the horizon as  $\delta_H = \varepsilon (M/M_0)^{-\gamma}$ , where  $M_0$  is the present horizon mass and  $n = 6\gamma + 1$ . To avoid having too much power on either large or small scales requires  $\gamma \approx 0$ , which corresponds to  $n \approx 1$ . Limits on the large-scale variation of the microwave background further imply  $\varepsilon \leq 10^{-4}$ . The case  $n = 1$  is commonly referred to as the constant curvature or (Harrison–Peebles–) Zeldovich<sup>59–61</sup> spectrum, and is predicted in inflationary models. It has recently been shown that not only inflation but also  $\varepsilon \approx 10^{-4}$  can be arranged in suitably fine-tuned grand unified theories<sup>62–64</sup>. The Zeldovich spectrum also arises automatically if the fluctuations are due to cosmic strings<sup>65,66</sup>. We show below that  $n = 1$  is, furthermore, in best agreement with galaxy and cluster data.

The first study of the growth of cold DM fluctuations was the numerical calculation of Peebles<sup>2</sup>, who included cold DM, photons, and ordinary matter. Two of us (G.R.B. and J.R.P.)<sup>3–5,7</sup> extended these numerical calculations to include three massless neutrino species. Fluctuations having mass  $M < M_{\text{eq}} = 2 \times 10^{15} (\Omega h^2)^{-2} M_{\odot}$  cross the horizon when the Universe is still radiation dominated, that is, when  $z > z_{\text{eq}} = 2.5 \times 10^4 \Omega h^2$ . After such fluctuations cross the horizon, their neutrino components dissipate by free streaming, and the remaining photon and charged particle perturbations oscillate as an acoustic wave (whose amplitude is ultimately damped by photon diffusion for<sup>67</sup>  $M < M_{\text{Silk}} \approx 3 \times 10^{13} \Omega_b^{-1/2} \Omega^{-3/4} h^{-5/2} M_{\odot}$ ). As a result, the main driving terms for the growth of cold dark matter fluctuations  $\delta_{\text{DM}}$  decrease, and consequently  $\delta_{\text{DM}}$  begins to grow only very slowly until the Universe becomes (dark) matter dominated at  $z_{\text{eq}}$ , after which  $\delta_{\text{DM}} \propto a = 1/(1+z)$  until  $z \approx \Omega^{-1}$ . This stagnation of the growth of DM fluctuations between the epochs of horizon crossing and matter domination is called 'stagnation'<sup>3–7</sup>.

Because fluctuations with  $M < M_{\text{eq}}$  grow very little during the stagspansion era and as fluctuations on all scales grow at essentially the same rate after the Universe becomes matter dominated, an initial Zeldovich spectrum,  $\delta_{\text{DM}} \propto M^{-2/3}$ , evolves to a much flatter spectrum for  $M < M_{\text{eq}}$  by the time of recombination. In Fig. 2 we plot the resulting cold DM fluctuation spectrum at present (ignoring the nonlinear evolution which is important for  $\delta \geq 1$ , as discussed below; thus the plotted spectrum  $\delta_k$  is larger than the spectrum at recombination by a constant factor). The quantity plotted in Fig. 2a,  $k^{3/2} |\delta_k|$ , roughly

represents the spatial density fluctuation  $\delta$  as a function of total mass  $M = 4\pi^4 \rho_0 / 3k^3$ . Also sketched are the fluctuation spectra in the hot DM scenario and in an isothermal scenario with white noise fluctuations. Note that the hot DM model requires more power on large scales today to form superclusters by  $z \approx 2$ . Figure 2b shows cold DM fluctuation spectra plotted in another form,  $\delta M/M$ , which represents the r.m.s. mass fluctuation within a randomly-placed sphere of radius  $R$  containing mass  $M$ . Following Peebles<sup>2</sup>, we have normalized the curves so that, at the present epoch,  $\delta M/M = 1$  at  $R = 8h^{-1}$  Mpc.

Even though baryonic fluctuations do not grow (and are damped for  $M < M_{\text{Silk}}$ ) before recombination, after recombination the baryons 'fall into' the DM perturbations so that quickly  $\delta_b = \delta_{\text{DM}}$  (refs 68, 69). This will occur if  $\Omega_{\text{DM}} \delta_{\text{DM}} \gg \Omega_b \delta_b$ , as we expect, and if the baryonic fluctuation mass exceeds the baryonic Jeans mass<sup>6</sup>  $M_{\text{J,b}} \sim 10^6 \Omega_b \Omega^{-3/2} h^{-1} (T_b/T)^{3/2} M_{\odot}$ , where  $T_b$  is the temperature of the baryonic gas and  $T$  is the photon temperature. On scales smaller than this, the pressure of the baryonic gas prevents it from developing the same density contrast  $\delta$  as the cold DM. The value of  $T_b/T$  is kept close to unity for  $z > 100$  by the coupling of the residual free electrons with the radiation, but for smaller  $z$  it falls off approximately as  $(1+z)$ . This means that at  $z \approx 10$ ,  $M_{\text{J,b}}$  may be as small as  $\sim 10^3 M_{\odot}$ .

At any mass scale  $M$ , when the fluctuation  $\delta M/M$  approaches unity, nonlinear gravitational effects become important. The fluctuation then separates from the Hubble expansion, reaches a maximum radius, and begins to contract. Spherically symmetric fluctuations, for example, contract to about half their maximum radii. During this contraction, violent relaxation due to the rapidly varying gravitational field converts enough potential energy ( $PE$ ) into kinetic energy ( $KE$ ) for the virial theorem,  $\langle PE \rangle = -2\langle KE \rangle$ , to be satisfied. After virialization, the mean density within a fluctuation is roughly eight times the density corresponding to the maximum radius of expansion<sup>8</sup>.

As the cold-DM fluctuation spectrum  $\delta M/M$  is a decreasing function of  $M$ , smaller mass fluctuations will, on the average, become nonlinear and begin to collapse at earlier times than larger mass fluctuations. Smaller mass fluctuations are themselves typically clustered within larger mass perturbations, which go nonlinear later. This hierarchical clustering of smaller systems into larger and yet larger gravitationally bound systems begins at the baryon Jeans mass,  $M_{\text{J,b}}$ , and continues until the present. The baryonic substructures within larger mass clusters will then be disrupted by virialization of the clusters unless significant mass segregation between baryons and DM has occurred before cluster virialization. Hence, to maintain their existence as a separate substructure, the baryons must cool and gravitationally condense within their massive DM haloes before virialization occurs on larger scales<sup>70</sup>.

Figure 3 shows the baryonic number density  $n_b$  plotted against temperature  $T$  (or halo velocity dispersion) for virialized spherically symmetric protocondensations resulting from an initial Zeldovich spectrum of cold DM fluctuations. The simplifying assumption of sphericity is not expected to be an unreasonable approximation for hierarchical clustering. Two cases are considered:  $\Omega = 1$  and  $h = 0.5$  (solid lines in Fig. 3), and  $\Omega = 0.2$  and  $h = 1$  (dashed lines). The curves assume that the protocondensations have virialized, but that the baryons have not yet cooled and condensed. The curves labelled  $1\sigma$  assume that for each mass scale,  $\delta M/M$  has the r.m.s. value; those labelled  $2\sigma$  correspond to fluctuations  $\delta M/M$  twice as great; and so on. For given total mass  $M$ , the distribution of values of  $\delta M/M$  spreads out along lines of constant  $M$  (light diagonal lines in Fig. 3). We have also shown in Fig. 3 the present positions of clusters and groups of galaxies and of individual galaxies, including dwarf spheroidals. Note that different types of galaxies, the Hubble sequence, are spread out in this diagram.

Baryonic cooling moves structures downward in Fig. 3, below the model curves. Baryons can radiatively cool through collisional excitation of atoms and molecules, and by Compton cooling off the cosmic background radiation; Fig. 3 correspondingly includes the medium solid curves labelled 'No metals' and

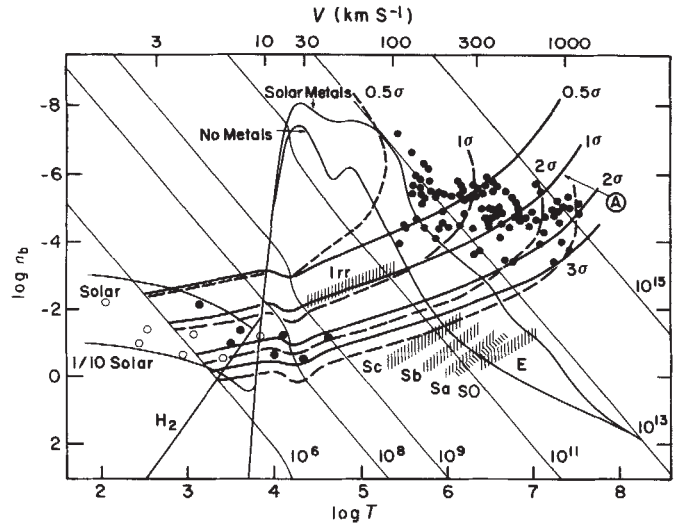


Fig. 3 Baryon density  $n_b$  versus three-dimensional, r.m.s. velocity dispersion  $V$  and virial temperature  $T$  for structures of various size in the Universe. The quantity  $T$  is  $\mu V^2/3k$ , where  $\mu$  is mean molecular weight ( $\approx 0.6$  for ionized, primordial H + He) and  $k$  is Boltzmann's constant. Dots at upper right represent nearly all groups and clusters within  $5,000 \text{ km s}^{-1}$  in the CfA catalogue<sup>82</sup>. Baryon density is obtained from total density assuming  $\rho_b/\rho = 0.1$  (see Table 1), where  $\rho$  is defined as  $M/(4\pi R_{\text{vir}}^3/3)$ ,  $M$  is total mass, and  $R_{\text{vir}}$  is  $GM/V^2$ . Catalogue groups are chosen to exceed a minimum threshold luminosity density. Their minimum baryon density should thus fall on a horizontal line, slightly modified by the higher  $M/L$  of rich clusters, as is observed. Point A represents Abell clusters of richness 2 and 3 studied by Dressler<sup>120</sup>. Here  $R_{\text{vir}} = 3.0 R_{\text{eff}}$ , valid for a de Vaucouleurs cluster profile<sup>125</sup>. The quantity  $T$  for clusters corresponds to central velocity dispersion, with the arrow indicating the effect of the falloff in velocity dispersion at large radii observed in the Coma cluster<sup>126,127</sup>. For galaxies,  $M_{\text{lum}}$  is set equal to  $(M_{\text{lum}}/L_B) \times L_B$ , where  $L_B$  is blue luminosity. Assumed values of  $(M_{\text{lum}}/L_B)$ : E = 8, S0 = 6, Sa = 4, Sb = 2.5, Sc = 1.5, Dw, Irr = 1.00, Dw. Spheroidal = 2.5 (all but the last are based on  $h = 0.5$ ). Galaxy radii are approximate virial radii, assuming that the baryonic components of galaxies are self-gravitating (to obtain a radius consistent with the definition used for groups and clusters above). To achieve this, isophotal radii from various sources have been appropriately scaled, as follows: E-Sb,  $R_{\text{vir}} = R_{25}$  (refs 128-131); Sc,  $R_{\text{vir}} = 1.24 R_{25}$  (ref. 132); Dw-Irr,  $R_{\text{vir}} = 1.24 R_H$  (ref. 133); Dw-Sph,  $R_{\text{vir}} = 0.70 R_{\text{id}}$  (ref. 51). Velocities: E-S0,  $V = \sqrt{3} \times \sigma$  (nucleus) (refs 129, 134); Sa-Sc,  $V = v_{\text{rot}}^{\text{max}}$  (refs 130, 131, 132); Dw-Irr,  $V = 1/2 \text{ FWHM } (\Delta v)$  (ref. 133), corrected for inclination. Dw Spheroidals are plotted twice; open circles,  $M = 2.5 L_B$  (stars only) and  $V = (GM/R_{\text{vir}})^{1/2}$ ; large dots,  $M = 30 L_B$  (stars plus dark matter<sup>48-51</sup>), with  $V$  as before. Light diagonal lines represent the masses of self-gravitating bodies with the indicated values of  $n_b$  and  $T$  and assuming  $\rho_b = 0.1 \rho$ . The discontinuities near  $10^4 \text{ K}$  are due to the effects of H and He ionization. Cooling curves<sup>78,135,136</sup> (medium lines) separate regions where cooling is efficient ( $\tau_{\text{cool}} < \tau_{\text{dyn}}$ , lower region) from regions where it is inefficient ( $\tau_{\text{cool}} > \tau_{\text{dyn}}$ , upper region). All curves assume a residual electron fraction after recombination of  $10^{-4}$ , consistent with  $\Omega_b/\Omega = 0.1$ . Model curves represent the equilibria of structures that collapse dissipationlessly from the cold dark matter initial fluctuation spectra of Fig. 2 with  $n = 1$ . DM haloes and groups and clusters of galaxies should lie on these curves, whereas the baryonic components of galaxies should lie below due to baryonic dissipation. The curves labelled  $\sigma$  refer to fluctuations with  $\delta M/M$  equal to  $\sigma$  times the r.m.s. value shown in Fig. 2. Heavy curves:  $\Omega = 1$ ,  $h = 0.5$ ; dashed curves:  $\Omega = 0.2$ ,  $h = 1$ . Model curves appear to pass through groups and clusters in about the right place, and the horizontal spread in  $T$  is roughly as expected for a gaussian distribution in  $\delta M/M$ . Baryonic components of galaxies lie below the loci for dissipationless collapse and generally within the region where strong baryonic cooling is expected. Dwarf spheroidal galaxies lie near the beginning of the clustering hierarchy and may be typical of the earliest structures to collapse (see ref. 73). Hubble types are spread out along different loci, perhaps due in part to different baryon collapse factors (Es larger, Irrs smaller) and in part to intrinsic differences in initial  $\delta M/M$  (see also Fig. 4).

'Solar metals', 'H<sub>2</sub>', and 'Compton'. Below these curves the baryonic cooling time is shorter than the dynamical time and above them the reverse is true<sup>71</sup>. Figure 3 immediately shows that, while the Hubble sequence of galaxies shows strong evidence for baryonic cooling and dissipation (core condensation in heavy haloes), dwarf spheroidals are only marginally able to cool, and groups and clusters of galaxies have too long a cooling time to have dissipated much energy on their scale<sup>72,73</sup>.

On average, for the cold DM fluctuation spectrum, what range of total masses yields baryon condensation within a massive halo? Let us first consider large galaxies. Naively, Fig. 3 suggests

that there is an upper bound for galactic masses of  $M \leq 10^{12} M_{\odot}$ , where the baryonic cooling time for gas of primordial composition begins to exceed the dynamical time. More massive galaxies could form in dense regions, where perhaps an early generation of Population III stars enriched the remaining baryonic gas with metals. Actually, the situation is likely to be more complicated, with many large galaxies formed by the merger of smaller ones. The resulting galaxy mass distribution arises from competition between hierarchical clustering and decreasing galaxy collision cross-sections due to dissipation, and it is thus difficult to calculate reliably. Regarding the smallest galaxies, collisional excitation of atomic hydrogen provides a lower limit of  $M \geq 10^8 M_{\odot}$ , corresponding to virialized baryonic temperature  $T_b \geq 10^4$  K. This range of protogalactic total masses,  $10^8 M_{\odot} \leq M \leq 10^{12} M_{\odot}$ , encompasses virtually all the mass that is observed to comprise galaxies. For protogalaxies in this mass range, the velocity dispersion of the baryons will initially remain nearly constant ( $T \approx \text{constant}$ ) as they condense within the gravitational potential of the virialized (and presumably roughly isothermal) DM halo. When the baryon density increases enough that their gravitational potential dominates that of the halo, the baryons' velocity dispersion will rise as they continue to dissipate energy and condense. Baryonic contraction is finally halted by rotation and perhaps, in some protogalaxies, by star formation (see below).

The collapse of fluctuations with mass  $M > 10^{13} M_{\odot}$  leads to clusters of galaxies in this picture. In clusters, only the outer parts of member galactic haloes are stripped off by collisions—the inner baryonic cores are able to contract to form the observed stellar systems. More of the baryons in the richest clusters are observed to be in the form of hot gas than in galaxies, as we have already mentioned in connection with Fig. 1. Perhaps this is because rich clusters tend to contain high-density cores, which collapse early, simultaneously with many of the galaxies they contain.

Can the cold DM picture account for the wide range of morphologies displayed by clusters of galaxies in X-ray<sup>74</sup> and optical-band<sup>75</sup> observations, ranging from regular, apparently relaxed configurations to complex, multicomponent structures? Preliminary results are encouraging. In particular, simulations show that large central condensations form quickly and can grow by subsequent mergers to form cD galaxies if most of the DM is in haloes around the baryonic substructures, as expected for cold DM, but not if the DM is distributed diffusely<sup>76,77</sup>.

What happens to small clouds whose baryonic mass  $M_b$  lies in the range  $M_{J,b} < M_b < 10^{7-8} M_{\odot}$  and for which  $T_b < 10^4$  K after virialization? For a primordial element abundance, the molecular cooling time (primarily due to  $H_2$ ) is less than the dynamical time for fluctuations that satisfy

$$M_b > M_{C,b} \approx 4.1 \times 10^6 (\Omega h^2)^{-0.917} \left( \frac{Y_e}{10^{-4}} \right)^{-0.625} \left( \frac{\Omega_b}{0.1\Omega} \right)^{-1.04} \\ \times \left( \frac{1+z_t}{10} \right)^{-2.75} M_{\odot}$$

where  $z_t$  is the redshift of maximum expansion of the fluctuation. (This result uses the cooling rates given by Yoneyama<sup>78</sup> and assumes the simple 'top hat' model of collapsing fluctuations. It corrects an equation given in ref. 17.) The quantity  $Y_e$ , the fraction of free electrons, is essentially the fraction that escapes recombination as the universe cools below  $\sim 1,000$  K, and is roughly  $10^{-4} (\Omega_b/0.1)^{-1} \Omega^{1/2} h^{-1}$ . Systems with  $M_b < M_{C,b}$  will persist as pressure supported clouds until they are disrupted by the virialization of larger scale clusters. Clouds having  $M_b > M_{C,b}$  can dissipate energy and collapse, although the influence of rotation and the efficiency of fragmentation are poorly understood. The end product may be an irregular or dwarf spheroidal galaxy. Other possibilities such as a protoglobular cluster or one or more very massive objects (VMOs) would require greater contraction and are likely to be inhibited by angular momentum.

Moreover, it is unclear what fraction of the original baryonic mass can be retained by such small clouds rather than expelled.

There is—despite the uncertainties—a strong probability that energy output from fragmented subsystems can influence the gas that remains uncondensed, thereby exerting a feedback on further condensation. In particular, UV emission from massive or supermassive stars can photoionize the remaining diffuse baryons, raising  $T_b$  up to  $10^4$  K. If such stars radiate a fraction  $q_{UV}$  of their Eddington luminosity in Lyman continuum photons, then the entire baryonic medium can be ionized even by a mass fraction of stars as low as  $\sim 3 \times 10^{-5} / q_{UV}$ . If the baryonic gas is re-ionized in systems with total mass  $M \leq 10^8 M_{\odot}$ , the baryons become so hot that they flow out of the cloud, whose gravitational field is not strong enough to bind them.

This may explain the origin of dwarf spheroidal galaxies, with  $10^6 M_{\odot} < M < 10^8 M_{\odot}$ , which show little evidence of dissipation in Fig. 3. As the baryons in these systems begin to condense through molecular cooling, if fragmentation and star formation are very efficient the baryons quickly turn into stars and condensation ceases. On the other hand, if a fraction of the baryons fragment into stars having strong UV luminosity, the remaining baryons are heated until they leave the system, and dissipation will again cease. The apparent absence of dissipation in dwarf spheroidals could also be due to stripping of their baryons in encounters with more massive systems<sup>32</sup>, which would move the dwarfs upward in Fig. 3.

In the cold DM scenario, globular clusters are probably not primordial objects. For one thing, there is no evidence that they have massive haloes (although, as Peebles<sup>79</sup> points out, there is not much direct contrary evidence either). Furthermore, if truly primordial, they should be distributed in the Universe like DM whereas, at least within galaxies, they seem to have dissipated and condensed like the other baryonic matter. However, the existence of 'standard objects' inside galaxies with mass  $\sim 10^6 M_{\odot}$  demands some explanation. In the model discussed here, there is a natural mass scale of order  $M_{g,b} \sim M_{Gal,b} (T_{virial}/10^4 \text{ K})^{-2}$ , where  $M_{Gal,b}$  is the baryonic mass within a galaxy;  $M_{g,b}$  is the Jeans mass of a cloud at  $10^4$  K in pressure balance with protogalactic gas at the virial temperature<sup>80</sup>. During the dissipation phase of galaxy formation, the gas might be likely to have a two-phase structure with a hot phase at  $T_{virial}$  and a cool phase at  $\sim 10^4$  K, in which case subcondensations of mass  $M_{g,b}$  would be expected with density contrast  $\approx T_{virial}/10^4$  K. We identify these with protoglobular clusters (noting that the considerations of Fall and Rees<sup>81</sup> could further limit the mass range).

## Galaxies and clusters

While the  $n_b$ - $T$  plot (Fig. 3) is useful for comparing data and predictions with the cooling curves, it is also useful to consider total mass  $M$  versus  $T$ , as in Fig. 4. This avoids having to take into account the differing amounts of baryonic dissipation suffered by various galaxies. The heavy solid and dashed curves again correspond to the  $n=1$  cold DM spectrum, for  $(\Omega=1, h=0.5)$  and  $(\Omega=0.2, h=1)$  respectively. It is striking that galaxies in the  $M$ - $T$  diagram lie along lines of roughly the same slope as these curves. This occurs because the effective slope of the  $n=1$  cold DM fluctuation spectrum in the galaxy mass range is  $n_{eff} \approx -2$ , which corresponds to the empirical Tully-Fisher and Faber-Jackson laws:  $M \propto v^4$ . The light dashed lines in Fig. 4 are the postvirialization curves for primordial fluctuation spectra with  $n=0$  (white noise) and  $n=2$ . The  $n=1$  (Zeldovich) spectrum is evidently the one that is most consistent with the data.

The points in Fig. 4 represent essentially all of the clusters identified by Geller and Huchra<sup>82</sup> in the CfA catalogue within  $5,000 \text{ km s}^{-1}$ . The cluster data lie about where they should on the diagram, and even the statistics of the distribution seem roughly to correspond to the expectations represented by the 0.5, 1, 2, and  $3\sigma$  curves. Note that the galaxies and clusters are neatly separated by the Compton cooling line of Fig. 3, suggesting that the era of galaxy formation ceased in the Universe when Compton cooling off microwave background photons became inefficient (J. E. Gunn, personal communication).

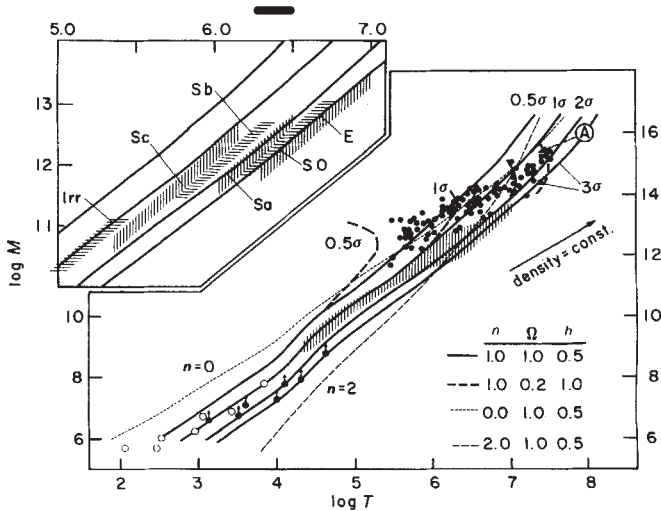


**Fig. 4** Total mass  $M$  versus virial temperature  $T$ . Data sources and symbols are as in Fig. 3.  $M$  for groups and clusters is total dynamical mass. For galaxies,  $M$  is assumed to be  $10 M_{\text{lum}}$  (see Fig. 3 legend). If  $Dw$  spheroidals actually have  $M/L_B = 30$ , they may have suffered baryon stripping<sup>32</sup>, in which case  $M$  is a lower limit (arrows). Details of the region occupied by massive galaxies are shown in the inset, upper left. In addition to the  $n=1$  models from Fig. 3, two  $1\sigma$  curves for  $n=0$  and  $n=2$  are also shown (light dashes). Either set of curves for an  $n=1$  (Zeldovich) spectrum provides a good fit to the observations over 9 orders of magnitude in mass. Curves with  $n=0$  and  $n=2$  do not fit as well. The apparent gap between galaxies and clusters in Fig. 3 (which stems from baryonic dissipation) vanishes in this figure, and the clustering hierarchy is smooth and unbroken from the smallest structures to the largest ones. The Fisher-Tully and Faber-Jackson laws for galaxies ( $M \propto V^4$  or  $T^2$ ) arise naturally as a consequence of the slope of the cold DM fluctuation spectrum in the mass region of galaxies. Groups and clusters are distributed around the  $n=1$  loci about as expected. The apparent upward trend among the groups is not physically meaningful but arises from their selection as density enhancements above a minimum threshold (see caption, Fig. 3, and constant-density arrow, this figure). The exact locations of galaxies are uncertain. In particular, the temperatures of Es and S0s may be overestimated owing to the use of nuclear rather than global velocity dispersions. The masses of  $Dw$  Irrs may also be too low owing to neglect of mass in  $H_2$ . Taken at face value, however, the data suggest that early-type galaxies (Es and S0s) arise from high- $\delta M/M$  fluctuations, whereas late-type galaxies (Scs and Irrs) arise from low- $\delta M/M$  fluctuations. Groups and clusters appear to fill a wider band than galaxies. If real, this difference may indicate that low- $\delta M/M$  fluctuations on the mass scale of galaxies once existed but did not give rise to visible galaxies. This suggests further that galaxy formation, at least in some regions of the Universe, may not have been fully complete and that galaxies are therefore not a reliable tracer of total mass. The sharp demarcation line between galaxies and clusters corresponds to the Compton cooling limit in Fig. 3 and suggests that galaxy formation ceased when Compton cooling off the microwave background became inefficient.

Note that spiral galaxies lie roughly along the  $1\sigma$  curve while elliptical galaxies lie along the  $2\sigma$  curve. Although this displacement is not large compared with the uncertainties, it is consistent with the fact that more than half of all galaxies are spirals, while only  $\sim 15\%$  are ellipticals. We have suggested elsewhere<sup>83</sup> that, in hierarchical clustering scenarios, the higher  $\sigma$  fluctuations will develop rather smaller angular momenta, as measured by the dimensionless parameter  $\lambda (=JE^{1/2}G^{-1}M^{-5/2})$ . This difference seems to exist with either white noise or a flatter spectrum, but to be larger in the latter case. If high  $\sigma$  fluctuations have little angular momentum, their baryons can collapse by a large factor in radius, forming high-density ellipticals and spheroidal bulges, as shown in Fig. 3. Because, with a flat spectrum, higher  $\sigma$  fluctuations occur preferentially in denser regions destined to become rich clusters (the statistics of such correlations can be treated<sup>84</sup> by the methods of Peebles<sup>6</sup>), one expects to find more ellipticals there—as is observed. Indeed, the rich clusters lie along the same 2 and  $3\sigma$  curves in Fig. 4 as do the elliptical galaxies.

Presumably the collapse of the low- $\lambda$  protoelliptical galaxies is halted by star formation well before a flattened disk can form, yielding a stellar system of spheroidal shape. The mechanism governing the onset of star formation in these systems is unfortunately not yet understood, but may involve a threshold effect which sets in when the baryon density exceeds the DM halo

density by a sufficient factor<sup>70,72</sup>. Disks (spirals and irregulars) form from more typical higher- $\lambda$  protogalaxies, which, for a given mass, are larger and more diffuse than their protoelliptical counterparts. The collapse of disks thus occurs through a relatively slow infall of baryons from  $\sim 10^2$  kpc, and is halted by angular momentum. Infall from such distances is consistent both with the extent of dark haloes inferred from observations and with the high angular momenta of present-day disks ( $\lambda \sim 0.4$ )<sup>85,86</sup>. The location of galaxies in Fig. 3 is consistent with these ideas if the baryons in all galaxies collapsed in radius by roughly the same factor, about an order of magnitude, but less for late-type irregulars and more for early-type Es and spheroidal bulges.

It has been theorized that the Hubble sequence originates in the distribution of either the initial angular momenta<sup>87,88</sup> or else the initial densities<sup>89</sup> of protogalaxies. However, if overdensity and angular momentum are linked, with the high- $\sigma$  fluctuations having lower  $\lambda$ , then these two apparently competitive theories become opposite sides of the same coin.

Consider finally the difference in Fig. 4 between the solid and dashed lines. The dashed lines, representing a lower-density Universe ( $\Omega = 0.2$ ), curve backward at the largest masses and lie far away from the circle representing the cores of the richest clusters, Abell classes 2 and 3. Because these regions of very high galaxy density contain at least several per cent of the mass in the Universe, the circle should lie between the 2 and  $3\sigma$  lines (assuming gaussian statistics). It does so for the solid ( $\Omega = 1$ ) lines, but not for the dashed lines. At face value, this is evidence favouring an Einstein-de Sitter Universe for cold DM. However, there are at least two reasons why this argument should not be taken too seriously. First, the velocity dispersions represented by the Abell cluster circle in Fig. 4 correspond to the cluster cores. The model curves on the other hand refer to the entire virialized cluster, over which the velocity dispersion is considerably lower (as indicated schematically by the arrow attached to the circle in Fig. 4). Second, the assumption of spherical symmetry used in obtaining both sets of curves is only an approximation. The initial collapse is probably often quite anisotropic—more like a Zeldovich pancake than a sphere. It is, therefore, preferable to compare these data with  $N$ -body simulations than with the simple model represented by the curves in Fig. 4. Until this becomes possible we do not believe that the data in Fig. 4 allow a clear-cut discrimination between the  $\Omega = 0.2$  and  $\Omega = 1$  cases, especially if the Hubble parameter  $h$  is allowed to vary simultaneously within the observationally allowed range, as we have assumed.

## Cosmological density

The most straightforward interpretation of the approximate constancy of  $M/M_{\text{lum}} \approx 10$  from galaxy through rich cluster scales (Fig. 1) is that dark matter clusters with galaxies. This is precisely what cold DM is expected to do. One then expects the density parameter  $\Omega = (M/M_{\text{lum}})\Omega_{\text{galaxies}} \approx 10 \times 0.02 = 0.2$ , in agreement with  $\Omega = 0.2 \times 1.5^{\pm 1}$  from the cosmic energy equation and the stability of clustering<sup>90</sup>.

The value  $\Omega \approx 0.2$  is consistent with all reliable measurements and furthermore gives an age for the Universe,  $t_0$ , consistent with globular cluster age estimates<sup>91</sup> ( $\geq 15$  Gyr) if  $h \leq 0.6$ . The observed abundance of deuterium plus helium-3 implies a lower limit<sup>37</sup>  $\Omega_b h^2 \geq 0.01$ , which is also consistent with  $\Omega = 0.2$  and  $\Omega_b \approx 0.02$  if  $h \geq 0.7$ .

Another argument favouring  $\Omega = 0.2$  for cold DM is based on preliminary  $N$ -body results<sup>92</sup>, which indicate that super-clusters and voids form on the observed scale for  $\Omega = 0.2$ , but on too small a scale for  $\Omega = 1$  unless the Hubble constant is unrealistically small. However, this conclusion follows from comparing the  $N$ -body mass autocorrelation function  $\xi_m(r)$  with the observed galaxy autocorrelation function  $\xi_g(r)$ . This is justified only if the galaxies are a good tracer of mass—if  $M/L \approx$  constant. This is certainly not true for rich clusters, as illustrated in the top part of Fig. 1 and in Table 1, where  $M/L$  for very rich clusters is roughly six times larger than it is for small groups

and for the Milky Way (including its DM halo). This means that some of the actual small-distance-mass autocorrelation is not included in the galaxy autocorrelation function; that  $\xi_m(r)$  is steeper for  $r \leq 1$  Mpc than  $\xi_g(r)$ . This effect is in the right direction to bring the  $\Omega = 1$   $N$ -body simulations into consistency with observations. Note that galaxy velocity dispersion averages also underestimate the actual mass-weighted velocity dispersion, because the high-velocity, dense regions of rich clusters are under-represented in the counts. This effect is also compatible with higher  $\Omega$ .

The absence of measurable fluctuations in the cosmic microwave background also restricts  $\Omega$ , because in a low- $\Omega$  Universe there is less growth of fluctuations both before and after recombination. The latest limits<sup>38,39</sup> on  $\Delta T/T$  require  $\Omega \geq 0.2h^{-4/3}$  (refs 93, 94), unless the Universe was reionized after recombination.

Both prejudice and the inflationary hypothesis favour the Einstein-de Sitter value  $\Omega = 1$ . (Actually, inflation implies more generally that  $\Omega = 1 - \Lambda/3H^2$ , where  $H$  is Hubble's constant and  $\Lambda$  is the cosmological constant<sup>95</sup>, but we assume here that  $\Lambda = 0$ .) For  $\Omega = 1$ ,  $t_0 = 6.5h^{-1}$  Gyr, so consistency with globular cluster age estimates requires the Hubble constant to be perhaps unrealistically small. As we have discussed, the Zeldovich ( $n = 1$ ) spectrum of primordial adiabatic fluctuations, which also follows from inflation, is compatible with models of galaxy formation in the cold DM scenario. Of course, the Zeldovich spectrum does not necessarily entail inflation. Moreover, inflation does not necessarily imply  $\Omega = 1$ : if there is a great deal of inflation, then, of course,  $\Omega$  is very close to unity (assuming vanishing cosmological constant); but if we speculate that greater amounts of inflation are increasingly unlikely, then our horizon might happen to lie in a patch with  $\Omega = 0.2$ .

Could  $\Omega = 1$  in the cold DM model? Based on Fig. 1, this could happen only if  $M/M_{\text{lum}}$  increases substantially on scales larger than rich clusters. Perhaps galaxy formation is suppressed in the voids, and the resulting luminosity contrast is so strong, for reasons we do not yet understand, that  $M/L > 1,500$  there (see below). Alternatively, if the virial mass of clusters of galaxies is significantly underestimated, as suggested recently by Kaiser, and if galactic haloes extend much further than  $\sim 70$  kpc, then the ratio  $M/M_{\text{lum}}$  may be substantially underestimated in Fig. 1, leading to a larger value for  $\Omega$ . If galaxy formation is inefficient so that only large-overdensity perturbations can form galaxies—a possibility suggested by Fig. 4—the  $\Omega = 1$ , cold DM  $N$ -body simulations<sup>92</sup> can be brought into agreement with observations<sup>96,97</sup>. We conclude that a straightforward interpretation of the evidence summarized above favours  $\Omega \approx 0.2$  in the cold DM picture, but that  $\Omega = 1$  is not implausible.

Note that the cold DM model may require some means of suppressing galaxy formation in voids for  $\Omega \approx 0.2$  as well as for  $\Omega = 1$ . This is required in the latter case to hide most of the mass. In a low- $\Omega$  Universe, on the other hand, large, very underdense regions cannot form by gravitation alone<sup>98,99</sup>; and galaxy formation must be suppressed somehow in regions of moderately low density if the density of galaxies in voids is less than one-quarter of the average density, the quoted upper limit for the Boötes void<sup>100,101</sup>. Suppression of galaxy formation may occur partly because of the substantial difference at  $z < \Omega^{-1}$  between  $\langle \rho \rangle$  and  $\rho_c$  in a low-density Universe.

## Superclusters and voids

Recent, accurate redshift measurements of several thousand galaxies have revealed the presence of voids with linear dimensions ranging up to  $\sim 50h^{-1}$  Mpc that are almost completely empty of bright galaxies. Most galaxies are concentrated in irregularly shaped, flattened, or elongated superclusters (see ref. 102 for fuller discussion and references). Two related observations are particularly interesting for their possible bearing on the origin of this large scale structure: a correlation of galaxy type with galaxy number density<sup>103,104</sup> and, possibly, a correlation between the orientation of cluster major axes and the direction to neighbouring clusters within  $\sim 15h^{-1}$  Mpc (ref. 105).

In the hot DM picture, the fluctuation spectrum is rather sharply peaked at masses  $\sim 4 \times 10^{15}$  ( $30 \text{ eV}/m$ )<sup>2</sup>. The suppression of smaller scale structure results in an essentially pressure-free collapse on the supercluster scale, with the formation of sharp caustics—Zeldovich pancakes<sup>106,107</sup>. If galaxies form only in the densest regions, where the shocked baryons have cooled sufficiently<sup>108,109</sup>, most of the Universe would be essentially devoid of galaxies. Simulations<sup>110</sup> also show large-scale cluster orientation correlations resembling those observed. On the other hand, the rapid evolution of the autocorrelation function requires that the pancakes form at  $z \leq 2$ , which is uncomfortably recent if smaller structures including galaxies must form subsequently.

The cold DM scenario avoids this latter problem because galaxies and clusters would already have formed by the time of supercluster collapse. Would superclusters and voids arise in a cold DM Universe? There are good reasons to believe that pancakes, filaments, and voids would indeed form, and preliminary indications from  $N$ -body simulations suggest that they do<sup>92,111</sup>. The cold and hot DM fluctuation spectra are identical on the very largest scales, differing only in that the latter is cut off below  $\sim 10^{15} M_\odot$  by neutrino free streaming and normalized larger above this scale (see Fig. 2a). The presence of already-formed and partially-virialized substructure in the cold DM case causes supercluster collapse to be less dissipative than in the neutrino picture because the caustics are thickened and because a smaller fraction of the baryons remains as cold, uncondensed gas. Nevertheless, as Dekel<sup>112</sup> has shown, persistent flattened or elongated structures can form even in the absence of dissipation as a result of continued expansion in directions orthogonal to the collapse. Indeed, the sharp caustics and highly dissipative shocks in the neutrino picture may produce superclusters that are too flat compared with the observations, even when gravitational interactions with neighbouring superclusters are taken into account.

Another related difference between hot and cold DM is that the hot DM Universe is predicted to have a rather simple cellular structure while the cold DM Universe probably has a considerably richer structure, perhaps more like that observed. In particular, the sizes of superclusters and voids in the cold case should span a fairly broad range. This will be an important test of the models when enough galaxy redshift data become available to indicate the statistics of the void distribution.

What should one expect to find in the voids? In the hot DM picture, all galaxies form from the dense gas along the caustics. Hence, the centres of voids should be entirely empty of galaxies and should contain only low-density DM and hot primordial gas (heated by radiation from pancake shocks and too dilute to have cooled)<sup>113</sup>. In the cold DM picture, one might at first suppose that galaxies form more or less uniformly in space, with their density subsequently enhanced by gravitational clustering and the pancake distortion of the Hubble flow. One would then expect to find galaxies in the voids, although with lower density than in superclusters.

In a low-density Universe, both analytical calculations<sup>98,99</sup> and  $N$ -body simulations<sup>92</sup> suggest that large regions having  $\rho/\langle \rho \rangle \leq 0.2$  cannot form by gravitational clustering alone. Nonetheless, large regions with few bright galaxies may actually be more likely in a low density cold DM Universe, for the following reason. On average, large galaxies form late when the average density has dropped well below the critical density. Larger initial fluctuations are thus required to form large galaxies in low-density regions. But larger fluctuations are statistically less likely in low-density regions with the flat, cold DM spectrum. This suppresses formation of large galaxies in moderate-size voids, and formation of clusters in larger voids<sup>84</sup>.

In addition, feedback from nongravitational processes could amplify the number density contrast of bright galaxies compared with the underlying density of dark and baryonic matter. For example, at  $z \sim 10$  the average density is highest where pancakes will later occur. This is where most of the earliest galaxies and rich clusters form, and these will be the regions earliest enriched

in metals. Radiation from these early galaxies (and quasars, and possibly Population III stars or VMOs) could heat the gas in lower density regions, raising the Jeans mass, as discussed above, and suppressing small galaxy formation. Indeed, if this early radiation has a hard enough spectrum and heats the gas sufficiently rapidly, it could raise the gas temperature throughout the Universe to  $10^6$  K and essentially halt galaxy formation outside pancakes. One of us (M.J.R.) has recently discussed<sup>114</sup> processes for suppressing galaxy formation in protovoids. Finally, explosive shocks could also enhance galaxy formation in denser regions<sup>115</sup>. Although the efficacy of all these processes is uncertain and needs further investigation, we conclude that the existence of large regions in which the density of bright galaxies is low is probably not a serious problem for the cold DM picture.

Now let us briefly discuss the two types of correlations mentioned above. The observed correlation of galaxy type with galaxy number density<sup>103,104</sup> can, at least partly, be understood as a consequence of the greater statistical likelihood of large- $\sigma$  fluctuations in regions of greater density (protoclusters), together with the effect discussed above that results in higher- $\sigma$  fluctuations acquiring lower angular momenta on average and becoming elliptical galaxies or spheroidal bulges. There is also an environmental effect: lower- $\sigma$  fluctuations yield dark haloes that are physically larger and more diffuse than higher- $\sigma$  fluctuations. Disks, which form from such fluctuations, thus form slowly, by infall of gas from large radii within these extended haloes. Because large haloes have correspondingly large collision cross-sections, few disks can form in regions of high galaxy number density. In dense regions, the halo gas is stripped by collisions and is mixed with enriched gas from galactic winds to become the hot intergalactic medium observed in X rays. It will be interesting to investigate these effects with  $N$ -body simulations and a more detailed theory of galaxy formation.

Regarding the second type of correlation, Binggeli<sup>105</sup> has found that the position angles of nearby, elongated Abell clusters are within  $45^\circ$  of the direction to the nearest cluster, provided the two clusters are separated by  $\leq 15h^{-1}$  Mpc. He found a similar, though less significant, correlation between the position angle of the brightest cluster galaxy's major axis and the direction to the nearest cluster. In the hot DM picture, where superclusters form before clusters and galaxies, such correlations arise naturally. Indeed an  $N$ -body simulation<sup>110</sup> has shown that such correlations also occur, but more weakly, even with a fluctuation spectrum having an adiabatic peak at  $\sim 10^{15} M_\odot$  superimposed on an  $n=0$  spectrum, so that rich clusters and superclusters form almost simultaneously. However, a preliminary analysis<sup>116</sup> of cold DM  $N$ -body simulations finds Binggeli-type correlations only if  $\Omega h \leq 0.2$ .

It is important to find other observationally accessible information that can discriminate between cosmological models. The large-scale velocity fields of superclusters should be rather different in the hot and cold DM schemes because of the much greater dissipation in the former. With new instruments it will also be possible to study the  $z < 2$  evolution of superclustering of quasars and of Ly $\alpha$  absorbing clouds, and perhaps the density and composition of the gas in voids.

It was once hoped that percolation analysis of the large scale galaxy distribution could help to distinguish between different cosmological models<sup>11,117</sup>. However, when this analysis is applied to the CfA galaxy data, the results are found to be a sensitive function of the depth of the survey<sup>118</sup>. Moreover, realistic  $N$ -body simulations of isothermal and adiabatic scenarios (that is, with accurate treatment of gravitational interactions on small as well as large scales) have nearly identical percolation properties<sup>110,119</sup>. Better statistical tests are needed to compare objectively the large-scale distribution of matter in models and observations.

## Conclusions

We have shown that a Universe with  $\sim 10$  times as much cold dark matter as baryonic matter provides a remarkably good fit

to the observed Universe. This model predicts roughly the observed mass range of galaxies, the dissipational nature of galaxy collapse, and the observed Faber-Jackson and Tully-Fisher relations. It also gives dissipationless galactic haloes and clusters. In addition, it may also provide natural explanations for galaxy-environment correlations and for the differences in angular momenta between ellipticals and spiral galaxies. Finally, the cold DM picture seems reasonably consistent with the observed large-scale clustering, including superclusters and voids. In short, it seems to be the best model available and merits close scrutiny and testing.

We thank Dick Bond, Jim Bardeen, Marc Davis, Avishai Dekel, George Efstathiou, Mike Fall, Carlos Frenk, Margaret Geller, Jim Gunn, Jim Peebles, Nicola Vittorio, and Simon White for valuable conversations. In addition, J.R.P. acknowledges the hospitality of the Max Planck Institute for Physics and Astrophysics, Munich during the summer 1983. This work was supported by the Department of Energy under contract no. DE-AC03-76SF00515 and by NSF grants AST-82-11551 and PHY-81-15541. This is Lick Observatory Contribution No. 436.

- Faber, S. M. & Gallagher, J. S. A. *Rev. Ast. Astrophys.* **17**, 135-187 (1979).
- Peebles, P. J. E. *Astrophys. J. Lett.* **263**, L1-L5 (1982).
- Primack, J. R. & Blumenthal, G. R. *Formation and Evolution of Galaxies and Large Structures in the Universe* (eds Audouze, J. & Tran Thanh Van, J. 163-183 (Reidel, Dordrecht, 1983).
- Primack, J. R. & Blumenthal, G. R. *4th Workshop on Grand Unification* (eds Weldon, H. A., Langacker, P. & Steinhart, P. J.) 256-288 (Birkhauser, Boston, 1983).
- Primack, J. R. & Blumenthal, G. R. *Clusters and Groups of Galaxies* (eds Mardirosian, F., Giuricin, G. & Mezzetti, M.) (Reidel, Dordrecht, in the press).
- Peebles, P. J. E. *Astrophys. J.* **277**, 470-477 (1984).
- Blumenthal, G. R. & Primack, J. R. Preprint (SLAC-PUB-3388, 1984).
- Peebles, P. J. E. *The Large Scale Structure of the Universe* (Princeton University Press, 1980).
- Efstathiou, G. & Silk, J. *Fundam. Cosmic Phys.* **9**, 1-138 (1983).
- Lyubimov, V. A. *et al. Phys. Lett.* **B94**, 266-268 (1980).
- Zeldovich, Ya. B., Einasto, J. & Shandarin, S. F. *Nature* **300**, 407-413 (1982).
- Shandarin, S. F., Doroshkevich, A. G. & Zeldovich, Ya. B. *Sov. Phys. Usp.* **26**, 46-76 (1983).
- Pagels, H. R. & Primack, J. R. *Phys. Rev. Lett.* **48**, 223-226 (1982).
- Olive, K. A. & Turner, M. S. *Phys. Rev. D* **25**, 213-216 (1982).
- Blumenthal, G. R., Pagels, H. & Primack, J. R. *Nature* **299**, 37-38 (1982).
- Bond, J. R., Szalay, A. S. & Turner, M. S. *Phys. Rev. Lett.* **48**, 1636-1639 (1982).
- Bond, J. R. & Szalay, A. S. *Astrophys. J.* **274**, 443-468 (1984).
- Ipser, J. & Sikivie, P. *Phys. Rev. Lett.* **50**, 925-927 (1983).
- Peccei, R. & Quinn, H. *Phys. Rev. D* **16**, 1791-1797 (1977).
- Weinberg, S. *Phys. Rev. Lett.* **40**, 223-226 (1978).
- Wilczek, F. *Phys. Rev. Lett.* **40**, 279-282 (1978).
- Preskill, J., Wise, M. & Wilczek, F. *Phys. Lett.* **120B**, 127-132 (1983).
- Abbott, L. & Sikivie, P. *Phys. Lett.* **120B**, 133-136 (1983).
- Dine, M. & Fischler, W. *Phys. Lett.* **120B**, 137-141 (1983).
- Fukugita, M., Watanabe, S. & Yoshimura, M. *Phys. Rev. Lett.* **48**, 1522-1525 (1982).
- Sikivie, P. *Phys. Rev. Lett.* **51**, 1415-1417 (1983); erratum **52**, 695 (1984).
- Ellis, J., Hagelin, J. S., Nanopoulos, D. V., Olive, K. & Srednicki, M. *Nucl. Phys. B* **238**, 453-476 (1984).
- Stecker, F. W. & Shafr, Q. *Phys. Rev. Lett.* **50**, 928-931 (1983).
- Freese, K., Price, R. & Schramm, D. N. *Astrophys. J.* **275**, 405-412 (1983).
- Carr, B. J. *Comments Astrophys.* **7**, 161-173 (1978).
- Lacey, C. G. *Formation and Evolution of Galaxies and Large Scale Structures in the Universe* (eds Audouze, J. & Tran Thanh Van, J.) 351-360 (Reidel, Dordrecht, 1984).
- Lin, D. N. C. & Faber, S. M. *Astrophys. J. Lett.* **266**, L21-L25 (1983).
- Canizares, C. R. *Astrophys. J.* **263**, 508-517 (1982).
- Witten, E. *Phys. Rev. D* **30**, 272-285 (1984).
- Carr, B. J., Bond, J. R. & Arnett, W. D. *Astrophys. J.* **277**, 445-469 (1984).
- Hegyi, D. J. & Olive, K. A. *Phys. Lett.* **126B**, 28-32 (1983).
- Yang, J., Turner, M. S., Steigman, G., Schramm, D. N. & Olive, K. A. *Astrophys. J.* (in the press).
- Uson, J. M. & Wilkinson, D. T. *Astrophys. J. Lett.* **277**, L1-L4 (1984).
- Uson, J. M. & Wilkinson, D. T. *Inner Space/Outer Space* (eds Kolb, E. W. *et al.*) (University of Chicago Press, in the press).
- Weinberg, S. *Astrophysical Cosmology: Proc. Study Week on Cosmology and Fundamental Physics* (eds Brück, H. A., Coyne, G. V. & Longair, M. S.) 503-528 (Pontifical Scientific Academy, Vatican, 1982).
- Kolb, E. W. & Turner, M. S. A. *Rev. Nucl. Part. Sci.* **33**, 645-696 (1983).
- Rees, M. J. *The Very Early Universe* (eds Gibbons, G., Hawking, S. & Siklos, S.) 29-58 (Cambridge University Press, 1983).
- Frenk, C., White, S. D. M. & Davis, M. *Astrophys. J.* **271**, 417-430 (1983).
- Dekel, A. & Aarseth, S. *Astrophys. J.* **283** (in the press).
- Kaiser, N. *Astrophys. J. Lett.* **273**, L17-L20 (1983).
- Faber, S. M. *Proc. 1st ESO-CERN Symp., Large Scale Structure of the Universe, Cosmology, and Fundamental Physics* (in the press).
- Bond, J. R., Szalay, A. S. & White, S. D. M. *Nature* **301**, 584-585 (1983).
- Aaronson, M. *Astrophys. J. Lett.* **266**, L11-L15 (1983).
- Aaronson, M. & Cook, K. *Bull. Am. astr. Soc.* **15**, 907 (1983).
- Cook, K., Schechter, P. & Aaronson, M. *Bull. Am. astr. Soc.* **15**, 907 (1983).
- Faber, S. M. & Lin, D. N. C. *Astrophys. J. Lett.* **266**, L17-L20 (1983).
- Davis, M., Lecar, M., Pryor, C. & Witten, E. *Astrophys. J.* **250**, 423 (1981).
- Hut, P. & White, S. D. M. *Nature* **310**, 637-644 (1984).
- Doroshkevich, A. G. & Khlopov, M. Yu. *Mon. Not. R. astr. Soc.* (in the press).
- Turner, M. S., Steigman, G. & Krauss, L. M. Preprint (Fermilab, 1984).
- Primack, J. R. & Roncadelli, M. Preprint (SLAC-PUB-3304, 1984).
- Shafr, Q. & Stecker, F. W. Preprint (Bartol Research Foundation, 1984).
- Gelmini, G., Schramm, D. N. & Valle, J. W. F. Preprint (CERN-TH.3865, 1984).
- Harrison, E. R. *Phys. Rev. D* **1**, 2726-2730 (1970).
- Peebles, P. J. E. & Yu, J. T. *Astrophys. J.* **162**, 815-836 (1970).
- Zeldovich, Ya. B. *Mon. Not. R. astr. Soc.* **160**, 1P-3P (1972).



62. Shafi, Q. & Vilenkin, A. *Phys. Rev. Lett.* **52**, 691-694 (1984).  
 63. Steinhilber, P. J. & Turner, M. S. Preprint (Fermilab, 1984).  
 64. Quinn, H. R. & Gupta, S. *Phys. Rev. D* **29**, 2791-2797 (1984).  
 65. Zeldovich, Ya. B. *Mon. Not. R. Astr. Soc.* **192**, 663-667 (1980).  
 66. Vilenkin, A. *Phys. Rev. D* **24**, 2082-2089 (1981).  
 67. Bond, J. R., Efstathiou, G. & Silk, J. *Phys. Rev. Lett.* **45**, 1980-1984 (1980).  
 68. Doroshkevich, A. G., Zeldovich, Ya. B., Sunyaev, R. A. & Khlopov, M. Yu. *Soviet Astr. Lett.* **6**, 252-256 (1980).  
 69. Chernin, A. D. *Soviet Astr.* **25**, 14-16 (1981).  
 70. White, S. D. M. & Rees, M. J. *Mon. Not. R. Astr. Soc.* **183**, 341-358 (1978).  
 71. Rees, M. J. & Ostriker, J. P. *Mon. Not. R. Astr. Soc.* **179**, 541-559 (1977).  
 72. Faber, S. M. *Astrophysical Cosmology: Proc. Study Week on Cosmology and Fundamental Physics* (eds Brück, H. A., Coyne, G. V. & Longair, M. S.) 191-234 (Pontifical Scientific Academy, Vatican, 1982).  
 73. Silk, J. *Nature* **301**, 574-578 (1983).  
 74. Forman, W. & Jones, C. *Ann. Rev. Astr. Astrophys.* **20**, 547-585 (1982).  
 75. Geller, M. J. & Beers, T. C. *Proc. Astr. Soc. Paci.* **94**, 421-439 (1982).  
 76. Thuan, T. X. & Romanishin, W. *Astrophys. J.* **248**, 439-459 (1981).  
 77. Cavaliere, A., Santangelo, P., Tarquini, G. & Vittorio, N. *Clusters and Groups of Galaxies* (eds Mardirossian, F., Giuricin, G. & Mezzetti, M.) (Reidel, Dordrecht, in the press).  
 78. Yoneyama, T. *Publ. Astr. Soc. Jap.* **24**, 87-98 (1972).  
 79. Peebles, P. J. E. Preprint (Princeton Univ., 1984).  
 80. Fall, S. M. & Rees, M. J. (in preparation).  
 81. Fall, S. M. & Rees, M. J. *Mon. Not. R. Astr. Soc.* **181**, 37P-42P (1977).  
 82. Geller, M. & Huchra, J. *Astrophys. J. Suppl.* **52**, 61-87 (1983).  
 83. Faber, S. M., Blumenthal, G. R. & Primack, J. R. *Astrophys. J. Lett.* (submitted).  
 84. Blumenthal, G. R., Faber, S. M. & Primack, J. R. (in preparation).  
 85. Efstathiou, G. & Jones, B. J. T. *Mon. Not. R. Astr. Soc.* **186**, 133-144 (1979).  
 86. Fall, S. M. & Efstathiou, G. *Mon. Not. R. Astr. Soc.* **193**, 189-206 (1980).  
 87. Sandage, A., Freeman, K. C. & Stokes, N. R. *Astrophys. J.* **160**, 831-844 (1970).  
 88. Efstathiou, G. & Barnes, J. *Formation and Evolution of Galaxies and Large Scale Structures in the Universe* (eds Audouze, J. & Tran Thanh Van, J.) 361-377 (Reidel, Dordrecht, 1984).  
 89. Gott, J. R. & Thuan, T. X. *Astrophys. J.* **204**, 649-667 (1976).  
 90. Davis, M. & Peebles, P. J. E. *Astrophys. J.* **267**, 465-482 (1983).  
 91. Sandage, A. *Proc. 1st ESO-CERN Symp., Large Scale Structure of the Universe, Cosmology, and Fundamental Physics* (in the press).  
 92. Davis, M., Efstathiou, G., Frenk, C. & White, S. D. M. (in preparation).  
 93. Bond, J. R. & Efstathiou, G. Preprint (NSF-ITP-84-79, 1984).  
 94. Vittorio, N. & Silk, J. Preprint (U. Cal. Berkeley, 1984).  
 95. Peebles, P. J. E. Preprint (Princeton Univ., 1984).  
 96. Kaiser, N. *Inner Space/Outer Space* (eds Kolb, E. W. et al.) (University of Chicago Press, in the press).  
 97. Bardeen, J. *Inner Space/Outer Space* (eds Kolb, E. W. et al.) (University of Chicago Press, in the press).  
 98. Hoffman, G. L., Salpeter, E. E. & Wasserman, I. *Astrophys. J.* **268**, 527-539 (1983).  
 99. Hoffman, Y. & Shaham, J. *Astrophys. J. Lett.* **262**, L23-L26 (1982).  
 100. Kirshner, R. F., Oemler, A., Schechter, P. L. & Schectman, S. A. *Astrophys. J. Lett.* **248**, L57-L60 (1981).  
 101. Kirshner, R. F., Oemler, A., Schechter, P. L. & Schectman, S. A. *Early Evolution of the Universe and its Present Structure, IAU Symp.* No. 104 197-202 (1983).  
 102. Oort, J. H. A. *Rev. Astr. Astrophys.* **21**, 373-428 (1983).  
 103. Dressler, A. *Astrophys. J.* **236**, 351-365 (1980).  
 104. Postman, M. & Geller, M. J. *Astrophys. J.* **281**, 95-99 (1984).  
 105. Binggeli, B. *Astr. Astrophys.* **107**, 338-349 (1982).  
 106. Zeldovich, Ya. B. *Astr. Astrophys. S.* **84**, 89 (1970).  
 107. Arnold, V. I., Shandarin, S. F. & Zeldovich, Ya. B. *Geophys. Astrophys. Fluid Dyn.* **20**, 111 (1982).  
 108. Bond, J. R., Centrella, J., Szalay, A. S. & Wilson, J. R. *Formation and Evolution of Galaxies and Large Structures in the Universe* (eds Audouze, J. & Tran Thanh Van, J.) 87-99 (Reidel, Dordrecht, 1984).  
 109. Shapiro, P. R., Struck-Marcell, C. & Melott, A. L. *Astrophys. J.* **275**, 413-429 (1983).  
 110. Dekel, A., West, M. J. & Aarseth, S. J. *Astrophys. J.* **279**, 1 (1984).  
 111. Melott, A., Einasto, J., Saar, E., Suisalu, I., Klypin, A. A. & Shandarin, S. F. *Phys. Rev. Lett.* **51**, 935-938 (1983).  
 112. Dekel, A. *Astrophys. J.* **264**, 373-391 (1983).  
 113. Doroshkevich, A. G., Shandarin, S. F. & Zeldovich, Ya. B. *Comm. Astrophys.* **9**, 265-273 (1982).  
 114. Rees, M. J. *Clusters and Groups of Galaxies* (eds Mardirossian, F., Giuricin, G. & Mezzetti, M.) (Reidel, Dordrecht, in the press).  
 115. Ostriker, J. P. *Astrophysical Cosmology: Proc. Study Week on Cosmology and Fundamental Physics* (eds Brück, H. A., Coyne, G. V. & Longair, M. S.) 473-493 (Pontifical Scientific Academy, Vatican, 1982).  
 116. Dekel, A. *8th Johns Hopkins Workshop on Current Problems in Particle Theory* (eds Domokos, G. & Kovesi-Domokos, S.) (World Scientific Publishing, Singapore, in the press).  
 117. Shandarin, S. F. *Soviet Astr. Lett.* **9**, 104 (1983).  
 118. Barrow, J. D. & Bhavsar, S. P. *Mon. Not. R. Astr. Soc.* **205**, 66 (1983).  
 119. Dekel, A. & West, M. J. Preprint (NSF-ITP-84-44, 1984).  
 120. Dressler, A. *Astrophys. J.* **226**, 55-69 (1978).  
 121. Jones, C. & Forman, W. *Astrophys. J.* **276**, 38-55 (1983).  
 122. Kriss, G. A., Cioffi, D. F. & Canizares, C. R. *Astrophys. J.* **272**, 439-448 (1983).  
 123. Beers, T. C., Geller, M. J., Huchra, J. P., Latham, D. W. & Davis, R. J. *Astrophys. J.* (in the press).  
 124. Gunn, J. E. *Astrophysical Cosmology* (eds Brück, H. A., Coyne, G. V. & Longair, M. S.) 233-259 (Pontifical Scientific Academy, Vatican, 1982).  
 125. Young, P. J. *Astr. J.* **81**, 807-816 (1976).  
 126. Kent, S. M. & Gunn, J. E. *Astr. J.* **87**, 945-971 (1982).  
 127. Kent, S. M. & Sargent, W. L. W. *Astr. J.* **88**, 697-708 (1983).  
 128. de Vaucouleurs, G., de Vaucouleurs, A. & Corwin, H. R. *2nd Reference Catalogue of Bright Galaxies* (University of Texas, Austin, 1976).  
 129. Dressler, A. & Sandage, A. R. *Astrophys. J.* **265**, 664-680 (1983).  
 130. Rubin, V. C. *Internal Kinematics and Dynamics of Galaxies* (ed. Athanassoula, E.) 3-6 (Reidel, Dordrecht, 1983).  
 131. Rubin, V. C., Ford, W. K., Thonnard, N. & Burstein, D. *Astrophys. J.* **261**, 439-456 (1982).  
 132. Burstein, D., Rubin, V. C., Thonnard, N. & Ford, W. K. *Astrophys. J.* **253**, 70-85 (1982).  
 133. Thuan, T. X. & Seitzer, P. O. *Astrophys. J.* **231**, 680-687 (1979).  
 134. Tonry, J. & Davis, M. *Astrophys. J.* **246**, 680-695 (1981).  
 135. Raymond, J. C., Cox, D. P. & Smith, B. W. *Astrophys. J.* **204**, 290-292 (1976).  
 136. Dalgarno, A. & McCray, R. A. A. *Rev. Astr. Astrophys.* **10**, 375-426 (1972).

## ARTICLES

# Ultrahigh gradient particle acceleration by intense laser-driven plasma density waves

C. Joshi\*, W. B. Mori\*, T. Katsouleas\*, J. M. Dawson\*,  
J. M. Kindel† & D. W. Forslund†

\* University of California Los Angeles, California 90024, USA

† Los Alamos National Laboratory, Los Alamos, New Mexico 87545, USA

*Space-charge waves driven by resonantly beating two laser beams in a high-density plasma can produce ultrahigh electric fields that propagate with velocities close to c. By phase-locking particles in such a wave, particles may be accelerated to very high energies within a very short distance.*

DURING the past four decades, we have witnessed an increase of six orders of magnitude in the output energy of high-energy accelerators, while the cost per MeV has been reduced by a factor of 16 per decade. But can this progress continue? Current accelerators, such as the Stanford linac, have accelerating fields of 200 keV cm<sup>-1</sup>. However, for particle energies beyond 10 TeV, one had to invent schemes that can produce fields of at least 10 MeV cm<sup>-1</sup>. In any particle accelerator scheme, the basic requirement for obtaining particles with ultrahigh energies is an intense longitudinal electric field that interacts with particles for a long time. Since highly relativistic particles move nearly at the speed of light *c*, the energy gained by the particles,  $\int E \cdot dl$ , is maximum if the field is made to propagate with the particles. Extremely large electric fields propagating with phase velocities close to *c* can be produced by space charge waves in a plasma (ionized gas). The maximum electric field that can be produced

by such a wave is approximately  $\sqrt{n_e}$  V cm<sup>-1</sup>, where  $n_e$  is the plasma electron density per cm<sup>3</sup>. Thus for plasma densities in the range 10<sup>16</sup>-10<sup>20</sup> electrons cm<sup>-3</sup>, the longitudinal electric fields  $E_L$  can be as large as 10<sup>8</sup>-10<sup>10</sup> V cm<sup>-1</sup>. We now show that such high-gradient, high-phase velocity plasma density waves can be driven by intense laser beams. If particles could be phase-locked in such waves, this scheme has the potential for accelerating particles to ultrahigh energies in very short distances.

## Theory

If an intense laser beam is propagated in a plasma, then in certain conditions, the transverse electric field of the laser (which may reach values of 10<sup>9</sup>-10<sup>10</sup> V cm<sup>-1</sup>) can be very effectively transformed into a longitudinal electric field of a plasma density wave. In the laser accelerator scheme known as the 'Plasma beat